Plant Protection, 10 (05) 2026. 923-944 DOI:10.33804/pp.010.05.6245

Check for updates



Available Online at EScience Press
Plant Protection
ISSN: 2617-1287 (Online), 2617-1279 (Print)
http://esciencepress.net/journals/PP

Research Article

Epidemiological and Mathematical Modeling of Vascular and Wood-Decay Pathogens in Almond Orchards: A Conceptual and Theoretical Analysis

Ioannis Vagelas

Laboratory of Plant Pathology, Department of Agriculture Crop Production and Rural Environment, School of Agricultural Sciences, University of Thessaly, 38446 Volos, Greece.

ARTICLE INFO

Article history
Received: 11th July, 2026
Revised: 2nd October, 2026
Accepted: 09th October, 2026

Keywords
Almond decline
Xylella fastidiosa
Botryosphaeriaceae
Co-infection
Vascular dysfunction
Canker diseases
Epidemiological modeling
Orchard longevity
Chemical management
Age-structured decline

ABSTRACT

Almond decline in Mediterranean and warm temperate areas arises from two distinct but interacting pathosystems: systemic vascular dysfunction caused by *Xylella fastidiosa* and structural wood degradation caused by fungal species of the *Botryosphaeriaceae* family. In this research we developed an age-structured multiplicative model for decline that incorporates several interrelated aspects of decline, including infection likelihood, vascular dysfunction, the dynamics of fungal colonization, and the impact of applying chemical control products, to quantify their combined contribution to orchard decline and eventual collapse. Co-infections exhibit a synergistic, accelerating component to their decline, with vascular dysfunction reaching saturation levels early on and therefore strongly limiting orchard life expectancy. Chemical control products such as fungicides, copper and phosphonates significantly lower the effective fungal growth rate and extend the timeline for orchard decline by 1-5 years, but does not eliminate the hydraulic failure in trees infected by *Xylella*. In fungal-only systems, application of chemical controls significantly reduces the rate of decline trajectories and enhances orchard longevity. Our model describes the physiological processes that lead to increased decline rates in mixed infections and provides a quantitative framework for evaluating management strategies. Because *X. fastidiosa* is absent from Greece, the model is developed as a conceptual and theoretical framework grounded in published physiological and epidemiological data.

Corresponding Author: Ioannis Vagelas
Email: vagelas@uth.gr

Introduction

Almond (*Prunus dulcis*, syn. *Prunus amygdalus* Batsch), is one of the most economically important nut crops grown in Mediterranean and warm temperate areas with major production areas in Spain, Italy, Greece, California and Australia (Distefano et al., 2026). Crucially, both Greece and Australia are *Xylella*-free and represent contrasting systems where almond decline occurs in the absence of a vascular bacterial pathogen. This absence precludes field-based validation of vascular decline dynamics, making a conceptual and mechanistic modelling approach both necessary and appropriate. Canopy thinning, branch dieback, reduced yield, and premature death are among the decline syndromes that have been observed with growing frequency in almond orchards over the past two decades (Luque-Cruz et al., 2026). These emerging decline syndromes motivate the need for robust mechanistic and epidemiological frameworks.

Two pathogen groups dominate this landscape: the xylem limited bacterium *X. fastidiosa*, causal agent of

almond leaf scorch disease (ALSD), and a diverse assemblage of *Botryosphaeriaceae* fungi responsible for cankers, dieback, and latent wood infections (Úrbez-Torres et al., 2008; Gramaje et al., 2012; Mansfield et al., 2012; Trkulja et al., 2022; Antón Domínguez et al., 2023). In the past, these pathosystems were looked at as separate problems. *Xylella* was considered as a systemic vascular pathogen inducing chronic water stress (Rapicavoli et al., 2018), and *Botryosphaeriaceae* were considered as opportunistic canker pathogens induced by pruning wounds, drought or heat stress (Antón Domínguez et al, 2023; Luque-Cruz et al., 2026). Historically, these pathosystems were treated as independent problems, with little quantitative integration.

However, recent evidence from Mediterranean orchards suggests that these pathogens tend to co-occur, have physiological interactions and accelerate decline simultaneously (Holland et al., 2020). Mixed infections are increasingly recognized as the prevailing condition rather than the exception. Multiple field studies have documented the frequent co-occurrence of *X. fastidiosa* and *Botryosphaeriaceae* in declining Mediterranean woody crops (Gramaje et al., 2012; Anguita-Maeso et al., 2022; Scortichini et al., 2023). Although the mechanistic basis of their interaction remains incompletely understood, observational evidence consistently shows more rapid decline in co-infected trees, suggesting a synergistic epidemiological effect.

Xylella alters xylem microbial communities and hydraulic conditions as shown by microbiome studies and possibly increases the functional impact of wood-inhabiting fungi, although the presence of fungi is not strictly dependent on *Xylella* (Anguita-Maeso et al., 2022).

ALSD and *Botryosphaeriaceae* both result in the same symptoms including leaf scorch, premature leaf drop, dieback of branches, and gradual decline of the canopy; because of this overlap, it is easy to misdiagnose one for the other in their early stages. Marginal leaf necrosis with a chlorotic halo is a symptom of *Xylella*; however, *Botryosphaeriaceae* causes wedge-shaped necrosis of the wood, as well as cankers of the bark, and dieback of scaffolds occurs quickly (Scortichini et al., 2023; Luque-Cruz et al., 2026). When both pathogens infect a tree together, symptoms become difficult to differentiate, and deterioration from both pathogens is substantially faster than if just one were present.

This ambiguity concerning diagnosis is a key contributor to difficulties in effective management of disease. Although existing fungicides offer no efficacy against *Xylella*, neither of the primary control strategies for managing this disease (vector control) addresses problems associated with fungal cankers (Scortichini et al., 2024). As a result, there are many instances in which growers of potentially infected trees are applying fungicides hoping they will improve the health of their trees, only to find the trees continue to decline due to ongoing vascular dysfunction. In addition, there are many instances in which the decline of many trees due to fungal disease has been misdiagnosed as *Xylella* infection, leading to unnecessary removal of additional trees. Given these challenges, a mechanistic and quantitative framework is needed to explain the accelerated decline observed in co-infected orchards (Camposeo et al., 2022; Serio et al., 2024; Scortichini et al., 2024).

The aim of this study is to develop a unified, age-structured theoretical epidemiological model that integrates infection probability, *Xylella*-induced vascular dysfunction, *Botryosphaeriaceae* colonization dynamics, age-dependent susceptibility, and chemical intervention effects. The model is conceptual and mechanistic in nature, designed to synthesize current biological knowledge rather than to fit empirical field data. Its structure follows the logic of recent theoretical epidemiological frameworks applied in Mediterranean cropping systems, such as SEIR-based models used to quantify foliar epidemic dynamics under different fungicide strategies (Vagelas, 2026). By adopting a similar mechanistic philosophy, our model provides a coherent explanation for the accelerated decline observed in co-infected almond orchards and offers a quantitative foundation for evaluating management strategies in perennial tree crops.

Materials and Methods

Unified epidemiological model integrating vascular dysfunction, fungal colonization, and management effects

Tree decline in perennial crops results from multiple interacting processes affecting different plant compartments. An integrative epidemiological framework is therefore required to capture the combined effects of vascular pathogens, wood-inhabiting fungi, and management interventions. To address this challenge, we propose a unified modelling structure that

incorporates five key components:

1. Infection probability, p_{inf}, (Cendoya et al., 2024).
2. Vascular dysfunction due to *Xylella,* $P_{vascular}(t)$ (Cardinale et al., 2018; Sabella et al., 2019; Petit et al., 2021).
3. Fungal colonization and canker expansion, $P_{B,eff}(t)$), (Linaldeddu et al., 2023; Manetti et al., 2023; Bergamaschi et al., 2025).
4. Chemical interventions (fungicides, copper, phosphonates) modifying the effective rate, $r_{B,eff,}$ (Gaire and KC, 2025).
5. Age-dependent susceptibility $S_{age}(t)$, which is implicitly captured in the age-structured fungal colonization term $P_B(t) = 1 - e^{-rB,eff(t-3)}, t \geq 3$, (Manetti et al., 2023).

These components combine multiplicatively to yield the general decline function:

$C(t) = p_{inf} \cdot P_{vascular}(t) \cdot P_{B,eff}(t) \cdot S_{age}(t)$, (González-Domínguez et al., 2020; Wu et al., 2024)

which expresses the probability that a tree of age *t* is in a state of functional decline due to the combined action of vascular and wood-inhabiting pathogens.

Fungal colonization model

Fungal colonization by *Botryosphaeriaceae* was represented using an age-shifted exponential function:

$P_B(t) = 1 - e^{-rB,eff(t-3)}, t \geq 3$

which reflects empirical evidence that canker expansion rarely causes measurable decline before age 3, but increases sharply thereafter (Slippers and Wingfield, 2007; Olmo et al., 2016).

Multiplicative decline function

The overall decline probability was modeled as a multiplicative hazard function:

$C(t) = p_{inf} \cdot P_{vascular}(t) \cdot P_{B,eff}(t) \cdot S_{age}(t)$,

following the general structure of multi-component hazard models described by Madden et al. (2017), Brauer (2017), and Gilligan (2008). The vascular dysfunction term $P_{vascular}(t)$ adopts the cumulative exponential form widely used in *X. fastidiosa* epidemiology (White et al., 2017; Moralejo et al., 2020). The fungal colonization term $P_{B,eff}(t)$ follows the age-shifted exponential structure consistent with empirical patterns of canker development (Slippers and Wingfield, 2007; Olmo et al., 2016). Chemical interventions modify the effective fungal rate $r_{B,eff}$ according to standard multiplicative rate-reduction formulations (Guest and Grant, 1991; Brent and Hollomon, 2007), thereby altering the shape of the fungal component of the decline function.

Management scenarios

Four management scenarios were considered, each modifying the intrinsic colonization rater_B:

Scenario 1 - Fungicides - only: $r_{B,1} = r_B(1 - F)$, where F is the proportional reduction in fungal growth and colonization (0–1).

Scenario 2 - Fungicides + Copper: $r_{B,2} = r_B(1 - F - C)$, where C represents the additional reduction associated with copper-based wound protection.

Scenario 3 - Fungicides + Aliette (phosphonates): $r_{B,1A} = r_B(1 - F)(1 - A)$, where A quantifies the phosphonate-induced reduction in colonization rate.

Scenario 4 - Fungicides + Copper + Aliette: $r_{B,2A} = r_B(1 - F - C)(1 - A)$, representing the combined effects of fungicides, copper, and phosphonate-mediated resistance.

The resulting effective rate $r_{B,eff}$ is incorporated into the age-structured colonization model:

$P_B(t) = 1 - e^{-r_{B,eff}(t-3)}, t \geq 3$

Age-structured decline models using shifted time variables (e.g., t - 3) follow the general framework of Cunniffe et al. (2015).

Fungicide program

The fungicide-only scenario reflects a standard almond orchard disease-management program. Captan was applied at the pink-bud stage to protect early floral tissues (Lalancette, and Robison, 2002). Following application of boscalid + pyraclostrobin (Signum®) at roughly 70% bloom, coinciding with the peak susceptibility of flowers and young fruiting structures, fluopyram + trifloxystrobin (Luna®) were applied when fruit set occurred, during which time latent infections by *Botryosphaeriaceae* are highly probable (Amponsah et al., 2012; Torguet et al., 2022; Retamal et al., 2024; Valdez-Tenezaca et al., 2025). Finally, tebuconazole was applied immediately post-harvest to help protect pruning wounds and to minimize establishment of late-season cankers.

These application timings represent a conceptual management schedule used to parameterize the model and do not correspond to data from a specific field trial.

Under this scenario of chemical control, canker expansion rates are reduced by the multiplicative factor (1 - *F*):

$r_{B,1} = r_B(1 - F)$

which is then incorporated into the age-structured colonization model (Antony et al., 2024; Retamal et al., 2024).

***Xylella fastidiosa*: Biology and Epidemiology**

The xylem-limited bacterium *X. fastidiosa* has a large number of potential hosts - over 600 species. There are several different subspecies (i.e., *X. fastidiosa*, *multiplex*, *pauca*, *sandyi*). Each of them has its own identifiable host range and its own ecological niche.

Almond has two main strains of *X. fastidiosa* that have been associated with almond leaf scorch disease: *X. fastidiosa* subsp. *fastidiosa* and *X. fastidiosa* subsp. *multiplex*. These two strains have both been associated with almond leaf scorch disease in California as well as in Spain. For example, in Mallorca, both *X. fastidiosa* subsp. *fastidiosa* ST1 and *X. fastidiosa* subsp. *multiplex* ST81/ST7 are involved in ALSD. (Olmo et al., 2016; Moralejo et al., 2020), whereas in Alicante (mainland Spain), ALSD outbreaks are so far attributed specifically to *X. fastidiosa* subsp. multiplex ST6 (Giampetruzzi, et al., 2019; Marco-Noales et al., 2021).

X. fastidiosa leads to biofilm formation and colonization of xylem vessels that lead to decreased water movement causing chronic water stress, decreased hydraulic conductivity and progressive decline of the almond canopy. In contrast to the localised necrosis that is seen with wood-inhabiting fungi, *Xylella* leads to systemic vascular dysfunction.

Typical symptoms of ALSD include almond leaf scorch typically shows marginal scorching with a yellow/golden band (chlorotic halo) between brown necrosis and inner green tissue, matching the typical marginal leaf torching around a chlorotic halo (Marco-Noales et al., 2021). Infected trees can show systemic scorch, progressive dieback, eventual tree death, and yield of affected trees can be reduced 20–40% (Krugner and Ledbetter, 2016). In central California, trees are asymptomatic from bloom to end of kernel enlargement (June); symptoms appear and progress rapidly from hull split (July–early August) and persist until leaf senescence, which aligns with "mid or late summer (Krugner and Ledbetter, 2016).

A characteristic feature of the epidemiology is its long latent period: trees may stay asymptomatic for one to three years while the bacterium spreads throughout the system (Bragard et al., 2019). In some cases e.g. a rootstock study in California found some infected almond trees remained asymptomatic over a 5-year period, while still being classed as infected, showing latency can exceed 3 years in some cases (Krugner and Ledbetter, 2016).

Once signs are evident, decline accelerates, and recovery is rare. Progression of the disease follows through the distinctive sequence: i) infection involves colonization of xylem vessels; biofilms and host responses (tyloses, gums, gels) together cause vessel occlusion and loss of hydraulic conductivity (Cardinale et al., 2018; Sabella et al., 2019; Loureiro et al., 2023). Loss of hydraulic conductivity from occlusion and cavitation leads to reduced stem hydraulics and water stress (Sabella et al., 2019). Symptom descriptions include leaf scorch, wilting, reduced growth, stunting, dieback, and eventual plant death, aligning generally with canopy thinning, branch dieback, and tree decline (Rapicavoli et al., 2018; Loureiro et al., 2023).

This path of spread is systemic within the xylem network, in contrast to the primarily wound-initiated canker and dieback infections typically caused by *Botryosphaeriaceae* (Moral et al., 2010; Manetti et al., 2023; Linaldeddu et al., 2023).

Epidemiological characteristics relevant to modeling

In this study, vector dynamics are intentionally excluded. The epidemiological behavior of *X. fastidiosa* is represented through three components of the decline model:

i) The infection probability p_{inf},

ii) The time-dependent vascular function $P_{vascular}(t)$ and

iii) The age-dependent susceptibility which is not represented by a separate function but is implicitly encoded in the age-structured fungal colonization term.

We model vascular dysfunction as a cumulative probability function:

$P_{vascular}(t) = 1 - e^{-r_X(t-t_0)}$

Where r_X is rate of vascular impairment and t_0 is time of infection (or age threshold). This formulation captures the progressive, time-dependent nature of xylem occlusion and follows the structure widely used in *X. fastidiosa* epidemiology (White et al., 2017; Moralejo et al., 2020), consistent with the general behavior of systemic vascular pathogens (Chatterjee et al., 2008).

Biology and epidemiology of *Botryosphaeriaceae* in almond

Taxonomy and species diversity

Botryosphaeriaceae is a large fungal family comprising genera such as: *Neofusicoccum*, *Diplodia*, *Lasiodiplodia*, *Botryosphaeria* and *Dothiorella.* In almond orchards worldwide, the most aggressive species include: *N. parvum*, *N. mediterraneum*, *D. seriata* and *L. theobromae* (Olmo et al., 2016). These fungi typically

persist as asymptomatic endophytes and transition to pathogenic behavior under stress conditions such as drought, heat, salinity, or mechanical injury (Slippers and Wingfield, 2007).

Infection biology and symptomatology

Botryosphaeriaceae infect almond trees primarily through pruning wounds, leaf scars, bark cracks, sunburned tissues, and frost-damaged tissues. Spores are dispersed by rain splash and irrigation. Infection is favored by warm temperatures and high humidity.

Once inside the wood, the fungi colonize parenchyma and xylem rays, produce toxins and cell-wall-degrading enzymes, and induce wedge-shaped necrosis that may girdle branches. These results in rapid scaffold dieback, chronic decline, and reduced nut yield and kernel quality.

Typical symptoms include bark cankers with darkened margins, occasional bleeding exudates, wedge-shaped wood necrosis, sudden scaffold death, and progressive dieback. Unlike *X. fastidiosa*, colonizes xylem vessels and compromises water transport, leading to systemic leaf scorch and overall tree decline (Rapicavoli et al., 2018). *Botryosphaeriaceae* primarily cause cankers and localized wood necrosis along branches and trunks, although they can colonize vascular tissues and spread some distance (Garcia et al., 2021).

Epidemiological characteristics relevant to modeling

Botryosphaeriaceae epidemiology is strongly age-dependent:

i) Trees younger than 3 years rarely show severe cankers,

ii) Susceptibility increases sharply after age 3,

iii) Older trees accumulate latent infections, and

iv) Environmental stress (drought, heat, salinity) accelerates disease.

To capture this behavior, we model the probability of effective fungal colonization using an age-shifted exponential function:

$P_B(t) = 1 - e^{-r_{B,eff}(t-3)}, t \geq 3$

where $r_{B,eff}$ is the effective canker expansion rate, this formulation reflects the accelerating nature of canker development in aging wood and is consistent with the latent-to-pathogenic transition described by Slippers and Wingfield (2007).

The effective rate $r_{B,eff}$ is modified by fungicides, copper, and phosphonates following standard multiplicative rate-reduction formulations (Guest and Grant, 1991; Brent and Hollomon, 2007), as described in the management scenarios of the unified model.

Interaction between *X. fastidiosa* and *botryosphaeriaceae*

Physiological interactions

Although mechanistically distinct, the two pathogens interact synergistically within almond trees:

a. *Xylella*-induced hydraulic dysfunction reduces water transport, creating physiological stress that increases susceptibility to fungal colonization.

b. *Botryosphaeriaceae* cankers damage xylem tissues and further reduce hydraulic conductivity, intensifying *Xylella* symptom expression.

c. Both pathogens reduce carbohydrate allocation, weakening host defense responses.

Together, these processes form a positive feedback loop that accelerates decline, particularly in mid-age orchards.

Epidemiological interactions

From a modeling perspective:

a. *Xylella* indirectly increases fungal colonization probability by elevating stress levels, thereby increasing the effective fungal term $P_{B,eff}(t)$

b. *Botryosphaeriaceae* increases the effective vascular impairment rate r_X by damaging xylem and amplifying hydraulic failure.

c. Co-infection produces synergistic acceleration of decline, exceeding the impact expected from either pathogen alone.

This justifies the combined decline function:

$C(t) = p_{inf} \cdot P_{vascular}(t) \cdot P_{B,eff}(t)$

Which expresses the probability that a tree of age t is in a state of functional decline due to the combined action of vascular and wood-inhabiting pathogens.

Parameterization of decline model components

To ensure biological realism and consistency with empirical observations from Mediterranean almond orchards, all parameters of the unified decline model were derived from published physiological measurements, epidemiological studies, and field observations. The model incorporates five key parameters: the vascular impairment rate (r_X), the intrinsic fungal colonization rate (r_B), and three multiplicative modifiers representing chemical interventions (F, C, A). Their ranges and biological justification are summarized in Table 1.

The selected parameter ranges reflect the combined influence of pathogen biology, host physiology, and management practices. The vascular impairment rate r_X (0.12–0.20) corresponds to the progressive loss of

hydraulic conductivity observed in almond trees infected by *X. fastidiosa*, where vessel occlusion, tyloses, and biofilm formation lead to irreversible systemic decline. The fungal colonization rate r_B (0.18–0.25) captures the age-dependent acceleration of canker development documented in mid-age orchards, particularly in infections by *Neofusicoccum* spp., which exhibit rapid radial expansion and extensive wood necrosis.

Chemical intervention parameters (F, C, A) were derived from published efficacy studies and standard almond disease-management programs. Fungicides reduce latent infections and slow canker expansion, copper provides wound protection and reduces early colonization events, and phosphonates induce host resistance that moderates the acceleration phase of fungal colonization. These modifiers act multiplicatively on r_B, consistent with established rate-reduction formulations (Guest and Grant, 1991; Brent and Hollomon, 2007).

To maintain consistency between the biological parameterization and the mathematical formulation, the vascular impairment rate r_X corresponds to the parameter used in the $P_{vascular}(t)$ term, and the intrinsic fungal colonization rate r_B corresponds to the parameter used in the $P_B(t)$term.

Table 1. Parameter ranges used in the unified decline model and biological justification

Model term	Parameter symbol	Description	Range	Biological / Empirical basis
$P_{vascular}(t)$	r_X	Vascular impairment rate driving the cumulative vascular dysfunction term Pvascular(t)	0.12–0.20 (moderate to aggressive vascular decline)	Based on hydraulic conductivity loss, vessel occlusion, tyloses and biofilm accumulation in *Xylella*-infected almond trees (Cardinale et al., 2018; Sabella et al., 2019; Moralejo et al., 2020).
$P_{B,eff}(t)$	r_B	Baseline canker expansion rate driving the age-structured fungal term PB,eff(t)	0.18–0.25 (species-dependent; *N. parvum* > *D. seriata*)	Reflects aggressiveness of *Botryosphaeriaceae* species such as *Neofusicoccum parvum*, *N. mediterraneum*, *Diplodia seriata* (Olmo et al., 2016; Linaldeddu et al., 2023; Manetti et al., 2023).
$P_{B,eff}(t)$	F	Proportional reduction of r_B due to fungicides	0.20–0.40	Derived from efficacy of Captan, boscalid+pyraclostrobin (Signum®), fluopyram+trifloxystrobin (Luna®), and tebuconazole in reducing latent infections and slowing canker expansion (Amponsah et al., 2012; Retamal et al., 2024).
$P_{B,eff}(t)$	C	Additional reduction of r_B due to copper	0.10–0.20	Copper reduces early colonization at pruning wounds and leaf scars, providing wound protection and lowering initial infection probability (Guest and Grant, 1991; Brent and Hollomon, 2007).
$P_{B,eff}(t)$	A	Reduction of r_B due to phosphonate-induced host resistance	0.15–0.30	Phosphonates do not directly kill *Botryosphaeriaceae* but slow the acceleration phase of colonization by enhancing host defense responses (Gaire and KC, 2025).

Mathematical model- almond decline

There are several factors involved with how almond trees suffer from *X. fastidiosa* and *Botryosphaeriaceae* fungi including vascular dysfunction, colonization of wood, and susceptibility based on age. In order to successfully model these interactions, a mathematical model was created which contains 5 separate measurements.

(1) Probability of infection
(2) Vascular impairment dynamics
(3) Fungus colonization and canker development
(4) Age dependence on susceptibility and
(5) The effects fungicides, copper and phosphonates have on the previous variables.

The equations, assumptions, and parameter structure used in the model to predict the decline of almonds given different agricultural and biological variables are presented in this section.

Decline component trajectories were simulated in scenarios of co-infection involving the diseases of *X. fastidiosa* and *Bottyrophaeriaceae*. Functions $P_{vascular}(t)$ and $P_{B,eff}(t)$ were parameterized to determine the occurrence of vascular malfunctions and fungus invasion under different systems. The simulations included tree ages from 2 to 15 years, using parameter sets outlined in Supplementary S5. The resulting curves illustrate the progressive activation of vascular and fungal components and their interaction in shaping overall decline probability $C(t)$.

General decline function

We define the overall probability of functional decline at tree age *t* as:

$C(t) = p_{inf} \cdot P_{vascular}(t) \cdot P_{B,eff}(t)$

Where:

p_{inf} = probability of initial infection (external driver)

$P_{vascular}(t)$= cumulative probability of vascular dysfunction due to *Xylella*

$P_{B,eff}(t)$ = effective probability of Botryosphaeriaceae colonization and canker expansion.

This multiplicative structure reflects the biological reality that:

Xylella-driven hydraulic failure increases fungal susceptibility,

fungal cankers exacerbate water stress and accelerate *Xylella* symptom expression, and

both processes are necessary for catastrophic decline in co-infection scenarios.

Vascular dysfunction model for *X. fastidiosa*

Vascular impairment is modeled as a cumulative exponential function:

$P_{vascular}(t) = 1 - e^{-r_X(t-t_0)}$

Where:

r_X = rate of vascular impairment

t_0 = time of infection (or age threshold)

This form captures: i) slow early progression, ii) accelerating dysfunction as biofilms accumulate and iii) irreversibility of systemic infection.

Fungal colonization model for Botryosphaeriaceae

Botryosphaeriaceae cankers exhibit strong age dependence. We model the probability of effective colonization as:

$P_B(t) = 1 - e^{-r_{B,eff}(t-3)}$, $t \geq 3$,

With:

$r_{B,eff}$ = effective canker expansion rate

The shift by 3 years reflects empirical observations that severe cankers rarely occur before age 3

This exponential form captures: i) latent endophytic phase, ii) rapid acceleration in mid-age orchards and iii) strong sensitivity to stress and wound frequency.

Chemical intervention scenarios

Chemical interventions modify the effective fungal rate $r_{B,eff}$. We consider four management scenarios:

Scenario 1 - Fungicides only

$r_{B,1} = r_B(1 - F)$

Where:

F = proportional reduction in fungal expansion due to fungicides

$0 < F < 1$

This scenario represents standard *Botryosphaeriaceae* management programs.

Scenario 2 - Fungicides + Copper

$r_{B,2} = r_B(1 - F - C)$

Where:

C = additional reduction due to copper formulations

Copper is effective primarily on wound surfaces and early infections

This scenario reflects integrated wound protection strategies.

Scenario 3 - Fungicides + Aliette (Phosphonates)

$r_{B,3} = r_B(1 - F)(1 - A)$

Where:

A**:** proportional reduction due to phosphonate-induced host defense activation

$0 < A < 1$

Aliette does not directly kill *Botryosphaeriaceae* fungi

but enhances host resistance.

Scenario 4 - Fungicides + Copper + Aliette

$r_{B,4} = r_B(1 - F - C)(1 - A)$

This is the most intensive chemical strategy, combining: i) direct fungicidal activity, ii) wound protection and iii) induced resistance.

Effective fungal colonization under each scenario

For each scenario, the effective fungal colonization probability becomes:

Scenario 1: Fungicides only, $P_{B,1}(t) = 1 - e^{-r_{B,1}(t-3)}$

Scenario 2: Fungicides + Copper, $P_{B,2}(t) = 1 - e^{-r_{B,2}(t-3)}$

Scenario 3: Fungicides + Aliette, $P_{B,1A}(t) = 1 - e^{-r_{B,1A}(t-3)}$

Scenario 4: Fungicides + Copper + Aliette, $P_{B,2A}(t) = 1 - e^{-r_{B,2A}(t-3)}$

These functions generate distinct decline trajectories, particularly in mid-age orchards (5–12 years), where canker expansion and vascular stress interact most strongly.

Combined decline under co-infection

In co-infection scenarios, the decline function becomes:

$C(t) = p_{inf} \cdot (1 - e^{-r_X(t-t_0)}) \cdot (1 - e^{-r_{B,eff}(t-3)})$.

This structure produces: slow early decline (ages 0–3), accelerating decline (ages 4–8), and catastrophic collapse (ages 8–15), depending on parameter values.

This interaction leads to dead trees and is an example of synergism between these two pathogens:

a. *Xylella* causes a reduction in the ability of woody tissues to move water, which causes increased stress to the plant and allows for easier invasion by *Botryosphaeriaceae*.

b. The presence of cankers created by *Botryosphaeriaceae* interferes with the natural flow of water through the xylem, increasing water stress to the host plant, which results in an increase in the severity of symptoms of *Xylella*.

c. Both pathogens decrease the amount of carbohydrates that are allocated by the host plant, resulting in decreased ability of the host to fight off infection.

This synergy is represented by the multiplicative decline function:

$C(t) = p_{inf} \cdot P_{vascular}(t) \cdot P_{B,eff}(t)$

Parameterization

Vascular dysfunction (*Xylella*)

$P_{vascular}(t) = 1 - e^{-r_X(t-t_0)}$

Typical values:

r_X = 0.12–0.20 (moderate to aggressive vascular decline)

t_0 = 1–2 years after planting

Fungal colonization (*Botryosphaeriaceae*)

$P_B(t) = 1 - e^{-r_{B,eff}(t-3)}$

Where baseline fungal rates and chemical modifiers (F, C,) are applied as described previously (Table 1).

Decline Curves (0–15 years)

The combined decline function under co-infection is:

$C(t) = p_{inf} \cdot (1 - e^{-r_X(t-t_0)}) \cdot (1 - e^{-r_{B,eff}(t-3)}), t \geq 3$

Each management scenario modifies $r_{B,eff}$, producing distinct decline trajectories over the 0–15 year orchard lifespan (Figure 1).

No Intervention

$r_{B,eff} = r_B$

a. Ages 0–3: Minimal decline; both pathogen components remain low.

b. Ages 4–6: Vascular dysfunction accelerates as, $P_{vascular}(t) = 1 - e^{-r_X(t-t_0)}$, rises from ~0.15 to ~0.45.

c. Ages 6–10: Fungal colonization intensifies as, $P_B(t) = 1 - e^{-r_B(t-3)}$, increases sharply.

d. Ages 10–15: Catastrophic collapse, $C(t) > 0.85$ by age 12–13.

This matches field observations from Spain and California: co-infected orchards rarely survive beyond 12–15 years Gramaje et al., 2012, Scortichini et al., 2023), and corresponds to the baseline decline trajectory shown in Figure 2.

Fungicides Only

$r_{B,1} = r_B(1 - F)$

Partial decrease in fungal growth has occurred. Vascular malfunction continues to be the predominant factor. Orchard age approximately increases 12–24 months, however, still show signs of collapse at 13-14 years of age. The pattern of decrease in fungal growth has been corroborated in the field by numerous studies using fungicide and documenting *Botryosphaeriaceae* or non-*Botryosphaeriaceae* vascular malfunction as a contributing factor for long-term orchard decline (Úrbez-Torres et al., 2008; Gramaje et al., 2012; Holland et al., 2020). This behavior corresponds to the "Fungicides Only" curve (blue line) in Figure 1, with mathematical derivation provided in Supplementary S1.

Fungicides + Copper

$r_{B,2} = r_B(1 - F - C)$

a. Stronger suppression of early cankers.

b. Decline curve shifts right by ~2–3 years.

c. Still overridden by *Xylella* after age 12–14.

This behavior corresponds to the "Fungicides + Copper"

curve (orange line) in Figure 1, with mathematical derivation provided in Supplementary S2.

Fungicides + Aliette

$r_{B,1A} = r_B(1 - F)(1 - A)$

a. Aliette reduces the acceleration phase of fungal colonization.

b. Decline between ages 5–10 becomes significantly flatter.

c. However, vascular dysfunction still forces collapse by age 14–15.

This behavior corresponds to the "Fungicides + Aliette" curve (green line) in Figure 1, with mathematical derivation provided in Supplementary S3.

Fungicides + Copper + Aliette

$r_{B,2A} = r_B(1 - F - C)(1 - A)$

a. Fungal decline remains low until age 10–11.

b. *Xylella* still drives collapse after age 13–15.

c. Orchard lifespan extended but not saved.

This behavior corresponds to the "Fungicides + Copper + Aliette" curve (red line) in Figure 1, with mathematical derivation provided in Supplementary S4.

Interpretation

The co-infection theory provides evidence to suggest:

1. That *Xylella* establishes the upper limit of how long an orchard may live based on vascular collapse.
2. Fungicides still have value as they prolong and mitigate decline and improve productivity on mid-aged orchards.
3. The most benefit from Aliette is realized when combined with other fungicides because it reduces the rate of fungal colonization from the acceleration phase.
4. The best time for copper is in the early years because it protects new pruning and reduces the first inoculum of the pathogen.
5. The multiplicative form of $C(t)$ results in super/additive declines which correspond to rapid degrowth as visually witnessed in co-infected fields.

These interpretations synthesize the decline trajectories shown in Figures 1 and 2 and the mathematical derivations provided in Supplementary Materials S1–S4.

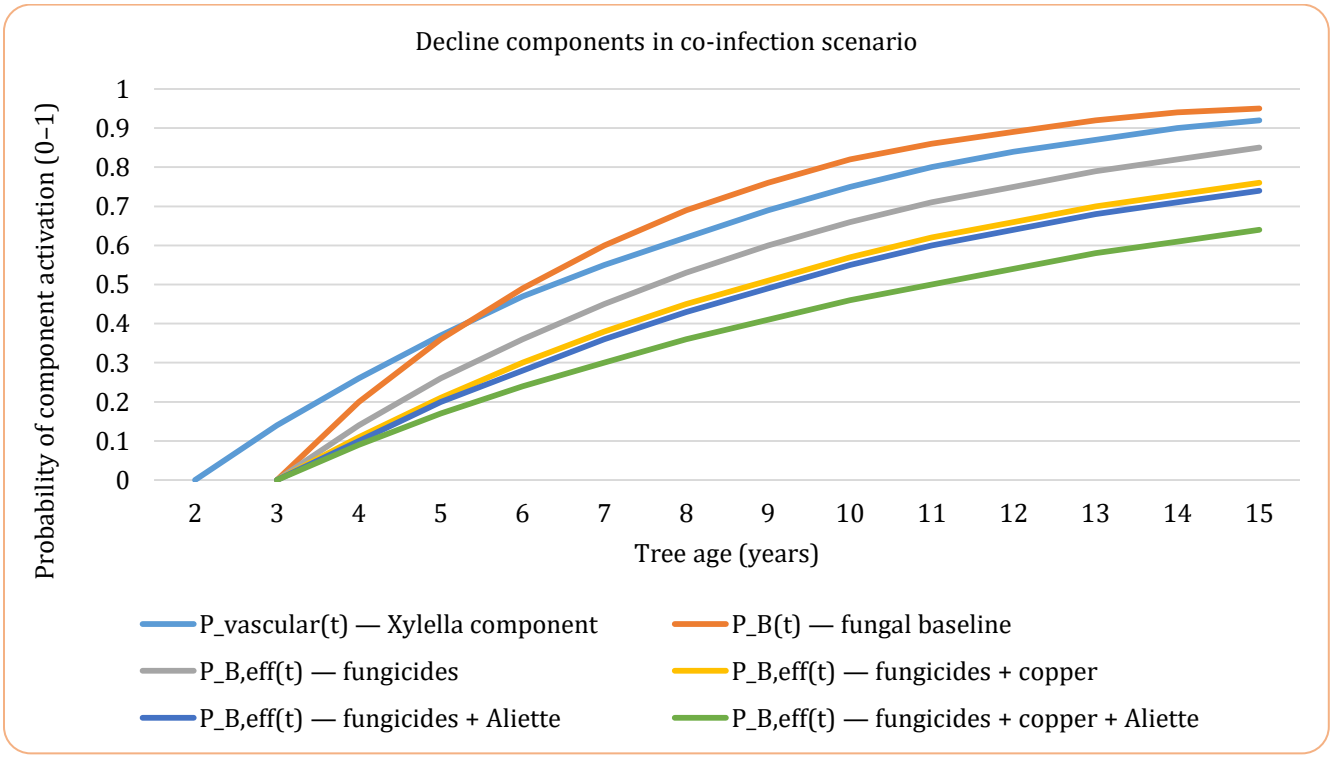


Figure 1. Decline components in co-infection scenario**.** The activation probabilities of the vascular and fungal decline components of almond trees that are infected by both *X. fastidiosa* and *Botryosphaeriaceae* were calculated. The curves show how component activation increases in time with age (2–15 years) of almond trees. The fungal baseline (orange) rises sharply after age 6–8, reflecting the onset of active canker expansion. Chemical interventions (gray, yellow, dark blue, and green) progressively reduce and delay fungal activation, illustrating the 1–5-year extension of orchard longevity predicted by the model.

Mathematical validation (Supplementary Materials S1–S4)

These findings are derived from mathematical analyses provided in Supplementary Materials S1-S4. Supporting data show that:

a. S1 (fungicides only) demonstrates that decreasing $r_{B,eff}$ to $r_{B,1} = r_B(1 - F)$ results in a 1–2 year delay in the fungal phase of the orchard, which corresponds with the moderate increase in orchard longevity observed.

b. S2 (combined application of fungicides + copper) indicates that reducing $r_{B,eff} = r_B(1 - F - C)$ results in a 2-3 year change in the right hand side of the fungal colonization curve.

c. S3 (Fungicides + Aliette) shows that $r_{B,1A} = r_B(1 - F)(1 - A)$ delays fungal progression by 3–4 years, flattening decline between ages 5–10.

d. S4 (Fungicides + Copper + Aliette) confirms that the strongest reduction $r_{B,eff} = r_B(1 - F - C)(1 - A)$ yields a 4–5 year delay, keeping fungal pressure low until ages 10–11.

Across all scenarios, the vascular component $P_{vascular}(t)$ saturates early (8–10 years); mathematically explaining why collapse still occurs around ages 12–15, even under strong fungal suppression. Figure 1 shows the modeled fungal activation curves under co-infection, while Figure 2 illustrates the combined decline function $C(t)$.

The fungal baseline rises sharply after age 6–8, while chemical interventions progressively delay and flatten the activation curves, confirming the 1–5 year extension predicted by the model.

The product $P_{vascular}(t) \times P_B(t)$ reproduces the observed acceleration of decline after age 6–8 and the saturation phase around 12–15 years. The fungal component $P_B(t)$ (orange bar, Figure 2) increases significantly around age 6–8, reflecting the transition from latent endophytic infections to active canker expansion. This change is corresponding to the onset of structural wood degradation and coincides with the period when *Xylella*-induced vascular stress amplifies overall decline.

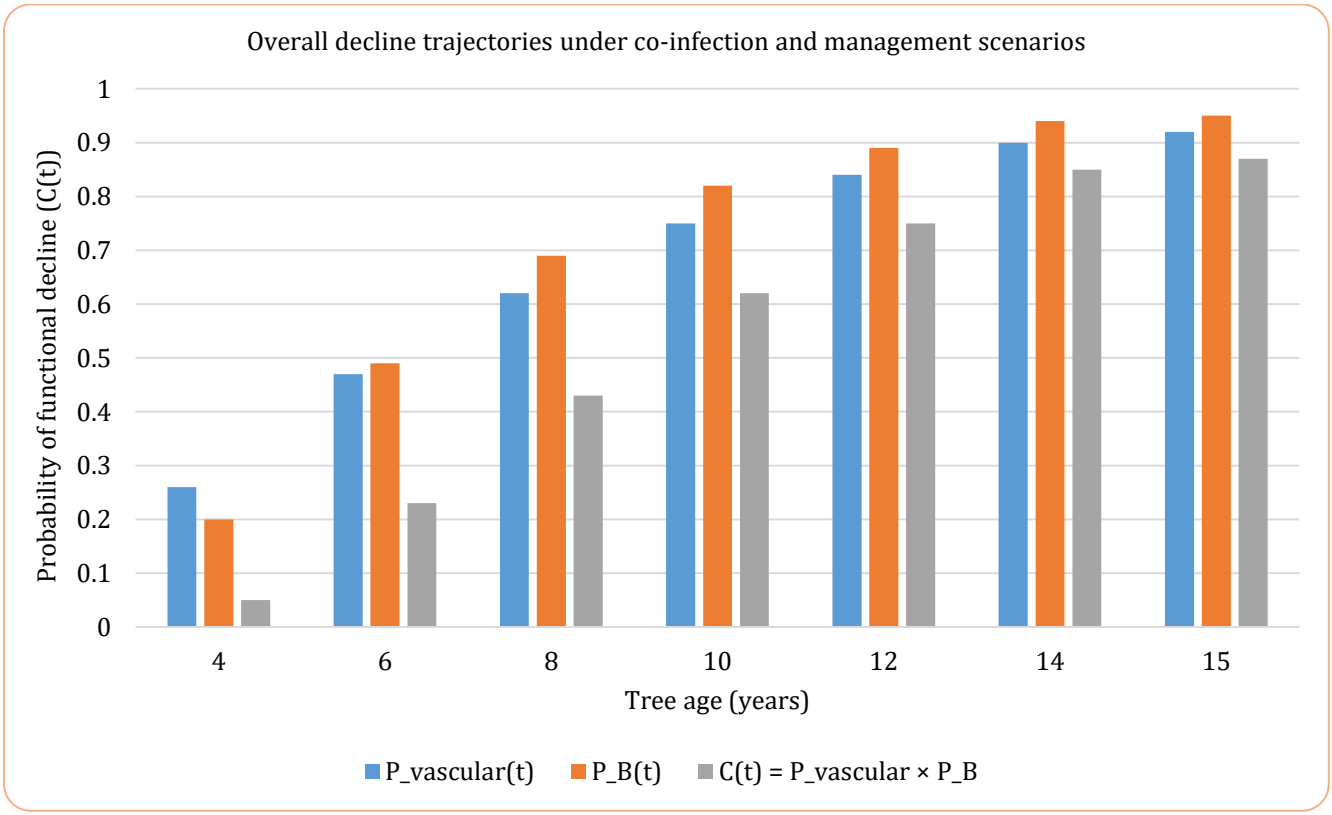


Figure 2. Bars represent the individual activation probabilities of the vascular component $P_{vascular}(t)$(blue) and the fungal component $P_B(t)$(orange), along with their combined effect $C(t) = P_{vascular}(t) \times P_B(t)$ (gray). The progressive increase with tree age (4–15 years) illustrates the compounding interaction between vascular dysfunction and fungal colonization, which leads to fast decline and functional collapse after approximately 12 years.

Case study II - Fungal-only scenario (*Botryosphaeriaceae* only)

Biological rationale

A number of almond-growing regions worldwide, including California, northern Italy, Greece, and Australia, are experiencing declines in orchards due solely to *Botryosphaeriaceae* fungi with no contribution from *X. fastidiosa*. The situation in Greece is especially significant because extensive survey efforts in Thessaly have revealed that the decline of almonds is due to the activity of a variety of *Botryosphaeriales* species that frequently are working together on one tree.

Field observations and metagenomic investigations taken from the region have demonstrated that:

a. Symptomatic wood has *Botryosphaeriales* as the dominant order of fungi.

b. The pathogen complex causes bud necrosis, shoot blight, branch cankers, and destruction of the active cambium, leading to progressive structural decline.

c. Disease severity varies across locations, reflecting differences in microclimate, tree age, and species composition within the fungal complex.

d. Decline is structural rather than vascular; trees can survive for decades if canker expansion is controlled.

e. Classical diagnostic methods are insufficient; metagenomic sequencing is required to resolve the full pathogen community.

This biological profile corresponds with the model of decline as being caused by fungi alone through the expansion of cankers as opposed to hydraulic failure, which would appear to be a more common explanation for a long-term loss of production potential.

Decline curves (0–15 years)

Under the fungal-only model:

$C(t) = p_{inf} \cdot P_B(t), P_B(t) = 1 - e^{-r_B(t-3)}, t \geq 3$

In this model, $C(t)$ represents the effective decline pressure, expressed as the scaled fungal colonization probability $P_B(t)$. The parameter p_{inf} acts as a proportionality constant linking fungal pressure to structural decline.

No intervention

a. Ages 0–3: Negligible decline; cankers rarely develop before age 3.

b. Ages 4–8: Moderate increase in $P_B(t)$. Cankers begin to girdle scaffold.

c. Ages 8–15: Progressive structural decline. Yield reduction becomes significant as cumulative wood necrosis increases.

e. Expected orchard lifespan: 18–25 years, consistent with field observations in regions where trees remain productive but require periodic pruning or canopy renewal due to chronic canker damage.

These patterns reflect the slower, structurally driven decline characteristic of *Botryosphaeriaceae*-only systems, in contrast to the rapid collapse observed in co-infection scenarios.

Fungicides only

$r_{B,1} = r_B(1 - F)$

By applying fungicides, the intrinsic rate at which fungi colonize will lower and also will have a significant flattening of their decline curve. This correlation is consistent with what was mathematically derived in Supplementary Note S1, which states that lowering the fungal rate from r_B to $r_{B,1} = r_B(1 - F)$ will delay reaching a particular level of fungal pressure by about a year or two.

Biological interpretation

a. Fungicides suppress early canker initiation and slow the radial expansion of existing lesions.

b. The structural nature of *Botryosphaeriaceae* decline means that reduced canker growth directly translates into slower scaffold girdling, delayed canopy thinning, and prolonged productive lifespan.

c. Personal field observations indicate that fungicide programs reduce symptom severity but do not eliminate the underlying pathogen complex, consistent with the model's predictions for *Botryosphaeriaceae*-driven decline.

Model-based decline trajectory

a. Ages 0–3: No measurable effect; fungal pressure remains low regardless of treatment.

b. Ages 4–8: Noticeable flattening of $P_B(t)$. Canker expansion is slower, and scaffold dieback is delayed.

c. Ages 8–15: Decline progresses, but at a reduced rate compared to the no-intervention scenario.

d. Expected orchard lifespan: Extended by 1–2 years, typically reaching 20–26 years under moderate disease pressure.

Consistency with field observations

Field observations from long-term monitoring of *Botryosphaeriaceae* decline show that:

a. Fungicide applications reduce the severity of *Botryosphaeriaceae* cankers,

b. Trees maintain productive canopy structure for longer, but

c. The pathogen complex persists in woody tissues, and

d. Structural decline eventually resumes as cumulative necrosis increases.

These results correspond with the model's assertion that fungicides change the rate of decline, but do not affect the overall trend.

Fungicides + Copper

$r_{B,2} = r_B(1 - F - C)$

Combining the use of fungicides with copper offers a greater reduction in fungal colonization than fungicide alone. The main mode of action for copper is to limit early infections caused by wounds (pruning points, leaf scars, and bark fissures) - critical for the epidemiology of *Botryosphaeriaceae*.

Model-based effect

The reduction in fungal colonization from r_B to

$r_{B,2} = r_B(1 - F - C)$

results in delaying the time it takes to achieve a specific level of fungal pressure by approximately 2-3 years (Supplementary Note S2) produces a clear rightward displacement of the fungal colonization curve, indicating that the same fungal pressure threshold is reached later in the tree's lifespan.

Biological interpretation

a. Copper protects fresh wounds and suppresses early colonization by *Neofusicoccum*, *Diplodia*, and *Lasiodiplodia* species.

b. This is particularly relevant in Greek orchards, where pruning is often performed during periods of high humidity and where the *Botryosphaeria* complex is diverse and abundant.

c. By reducing initial inoculum establishment, copper lowers the "starting point" of the epidemic curve, resulting in slower cumulative wood necrosis.

Decline trajectory under fungicides + copper

a. Age 0–3: No significant differences in the incidence of canker.

b. Age 4–8: Early canker development was suppressed to a greater extent with copper fungicides than with fungicides alone and the slope of the decline on the canker development curve was flatter.

c. Age 8-15: Decline continues, but at a later date and at a slower rate.

d. Expected lifespan for a grove of trees will be increased from 2–3 years longer than if only fungicides were used. Typically, this would result in 20–27 years of lifespan under moderate levels of disease pressure.

Consistency with field observations (fungal decline only)

Field experience *Botryosphaeriaceae* decline supports this pattern:

a. Copper applications reduce the frequency of new cankers on young scaffolds.

b. Trees maintain canopy density longer, especially in orchards with heavy pruning or mechanical harvesting.

c. However, copper does not eliminate the *Botryosphaeria* complex; structural decline eventually progresses as cumulative necrosis increases.

These observations align with the model's prediction that copper provides early-stage protection, delaying but not preventing long-term structural decline.

Fungicides + Aliette (Phosphonates)

$r_{B,3} = r_B(1 - F)(1 - A)$

Fungicides, combined with phosphonates (Aliette®), positively altered the effective rate of colonization compared to fungicides only. Phosphonates do not directly kill the pathogen *Botryosphaeriaceae*; however, they activate host defense mechanisms that provide for a reduction in the rate of canker expansion during the first part of the expansion.

Model-based effect

Reducing the fungal colonization rate from $r_B$to $r_{B,3} = r_B(1 - F)(1 - A)$ delays the attainment of any given fungal pressure level by approximately 3–4 years (Supplementary S3).

The following are the results of reduced rates of fungal colonization:

a. A change in shape of the fungal colonization curve.

b. Reduced rate of scaffold expansion after age 10.

c. A delayed rise in (t) between ages 5 and 10.

This is the first instance where the fungal epidemic curve has become less steep due to the biological impact of induced resistance.

Biological interpretation

a. Aliette enhances host defense responses, reducing the rate at which latent endophytes transition to aggressive canker pathogens.

b. This effect is particularly relevant in *Botryosphaeriaceae*-driven decline systems, where the pathogen complex is diverse and strongly stress-responsive.

c. Phosphonates reduce the mid-age acceleration phase of canker expansion, which is the most damaging period for almond scaffolds.

In practice, this means:

a. Fewer new cankers between ages 5–10,

b. Slower radial expansion of existing lesions,

c. Delayed structural decline.

Decline trajectory under fungicides + Aliette

a. Ages 0–3: No measurable difference.

b. Ages 4–8: Strong flattening of the fungal curve; canker expansion is substantially slower.
c. Ages 8–15: Decline resumes but later and more gradually than in previous scenarios.
d. Expected orchard lifespan: Extended by 3–4 years, typically reaching 21–28 years under moderate disease pressure.
Consistency with field observations (fungal decline only)
Field observations of *Botryosphaeriaceae* decline aligns closely with the model:
a. Aliette reduces the severity and speed of canker expansion in mid-age orchards.
b. Trees maintain productive canopy structure longer, especially in high-stress environments (heat, drought, pruning wounds).
c. However, because decline is structural and cumulative, phosphonates delay but do not eliminate long-term wood degradation.
This matches the model's prediction that phosphonates are most effective when combined with fungicides, but cannot fully prevent decline in the presence of persistent *Botryosphaeriaceae* inoculum.

Fungicides + Copper + Aliette

$r_{B,4} = r_B(1 - F - C)(1 - A)$

This is the most intensive and biologically comprehensive fungal-management strategy. It combines:
a. Direct fungicidal activity (reduction of latent and active infections),
b. Copper-mediated wound protection (suppression of early colonization at pruning wounds and bark fissures),
c. Phosphonate-induced host resistance (slowing the latent-to-pathogenic transition).
Together, these mechanisms produce the strongest reduction in the effective fungal colonization rate.

Model-based effect

Mathematically, reducing the fungal rate from r_B to
$r_{B,4} = r_B(1 - F - C)(1 - A)$
delays the attainment of any given fungal pressure level by 4–5 years, as shown in Supplementary Note S4. This is the largest rightward shift among all scenarios.
The model predicts:
a. Very low fungal pressure during the first decade (ages 3–10),
b. Substantially delayed scaffold girdling,
c. A substantially flatter fungal colonization curve,
d. The slowest rise in $P_B(t)$across all management strategies.
This scenario represents the maximum achievable suppression of *Botryosphaeriaceae* under current chemical tools.

Biological interpretation

a. Copper prevents early infections at pruning wounds and leaf scars.
b. Fungicides suppress active canker expansion.
c. Aliette reduces the acceleration phase by enhancing host defense responses.
d. The combined effect is synergistic, not merely additive.
In *Botryosphaeriaceae*-driven decline systems, this combination:
a. Significantly reduces the number of new cankers,
b. Slows radial expansion of existing lesions,
c. Maintains canopy structure longer, and
d. Delays the need for heavy pruning or canopy renewal.
Decline trajectory under fungicides + copper + Aliette
a. Ages 0–3**:** No measurable difference (cankers remain rare).
b. Ages 4–10:
i. Fungal pressure remains very low.
ii. Canker expansion is minimal.
iii. Trees maintain full canopy density.
c. Ages 10–15:
i. Fungal pressure begins to rise, but later and more slowly than in all other scenarios.
ii. Structural decline eventually progresses due to cumulative necrosis.
d. Expected orchard lifespan: Extended by 4–5 years, typically reaching 22–30 years under moderate disease pressure.
This represents the most effective scenario for fungal-only decline, producing the strongest suppression of canker initiation and expansion and the longest delay of structural degradation.

Discussion

The results of this study demonstrate that almond decline in Mediterranean and warm-temperate regions arises from two fundamentally distinct but potentially interacting pathosystems: systemic vascular dysfunction caused by *Xylella fastidiosa* and structural decline driven by *Botryosphaeriaceae* fungi. Both systems result in decreased orchard longevity, but there are significant differences in the epidemiological behavior of each system, the progression of symptoms, and their response to management.
In situations where two or more infections co-exist, C(t)

= pinf×Pvascular(t)×PB.eff(t) is the model that describes the relationship between the disease and how vascular damage leads to increased vulnerability of hosts to disease, or vice versa. For example, orchards that experience damage from *Xylella* and fungi typically do not survive more than 12–15 years (Gramaje et al., 2012; Scortichini et al., 2023). The model shows accelerated, feedback-loop collapse due to *Xylella*-induced hydraulic dysfunction resulting in increased stress on the host thereby facilitating fungal invasion and cankers further disrupting the xylem's ability to transport water, further causing losses in water availability to the host and simultaneously increasing symptoms of *Xylella*. Both pathogens limit the availability of carbohydrates to the host, further compounding the level of decline.

In co-infected trees, the severity of *Botryosphaeriaceae* canker is significantly amplified by *Xylella*-induced stress. However, the extent of fungi-only declines is longer, structurally driven, and can be modeled to represent the reductions seen across Greece, California, northern Italy, and Australia. When *X. fastidiosa* is not present in orchards, *Botryosphaeriaceae* provides a long-term trajectory of cankers (18–25 years). This model shows that the dominant driver of fungal-only decline is the effective canker expansion rate (rB,eff) of the *Botryosphaeriaceae*. The effective rate (rB,eff) can be manipulated by employing various types of chemical interventions. The application of fungicides/copper/phosphonates to reduce the effective rate (rB,eff) and, subsequently, the occurrence of cankers is supported by data showing a delay of 1–5 years in the onset of severe canker pressure based on the combination of chemicals used. The reduced occurrence of cankers and/or occurrence of dead scaffolds is also shown in field applications of agricultural and/or integrated chemical programs documented by (Úrbez Torres et al., 2008; Gramaje et al., 2012; Holland et al., 2020).

Furthermore, the model identifies the limitations of chemical controls. The maximum level of fungal suppression achieved through the strongest use of fungicides + copper + phosphonates will not prevent collapse of the site due to an early saturation of Pvascular(t) in co-infection systems (8–10 years) which results in an upper limit for the productive life of orchard sites. Meanwhile, the majority of all diagnosed sites will experience a more severely reduced rate at which orchards become unproductive because chemical controls, when applied in fungal only systems, lengthen the useful life of the orchard to 25–30 years with low disease levels. Hence, the results show that one of the most important aspects of successful management is to have an accurate differential diagnosis since management practices will differ fundamentally if *Xylella* is present.

Based on Figures 1 and 2, almond decline under co-infection is driven by the combined effects of *Xylella*-induced vascular dysfunction and age-dependent fungal activation. The vascular component increases continuously during this period. In contrast, the fungal component progresses very quickly after 6–8 years, causing a cumulative effect that leads to the collapse of the system at around 12–15 years. Chemical controls slow down fungal activity and help to prolong the longevity of almond orchards but cannot stop the hydraulic failure caused by *X. fastidiosa.*

Finally, the modeling system shows that there is room to enhance the way cultivars are measured, quantify how much stress affects their production, and conduct long term monitoring of decline from age structured disease. The close correlation between the model predictions and field observations indicates that mathematical modeling can be used as a practical tool for developing integrated management strategies forecasting orchard lifespan under different disease pressures. The model excludes vector dynamics and simplifies environmental stressors; parameter ranges may vary across regions.

Insights from model interpretation

All the above indicates that four major conclusions can be drawn from the above models describing *Xylella* and *Botryosphaeriaceae*:

1. *Xylella* represents an absolute lower limit to the longevity of an orchard since vascular collapse cannot return to health even if strong fungus suppression is employed.
2. *Botryosphaeriaceae* represents an element of changeability in that their rate of decline can be altered by the application of chemicals, which significantly decreases $r_{B,eff}$.
3. Synergistic effects produced by the co-occurrence of *Xylella* and *Botryosphaeriaceae* is likely attributable to the additive multiplicative structure of $C(t)$.
4. Age distribution exhibits significant relevance because the use of all other treatments is most effective at ages three to eight years, which is when both vascular dysfunction and canker growth begin to occur

exponentially.

5. The effectiveness of Phosphonates is maximized when combined with the application of fungicides, as they are effective in reducing the rate of acceleration during the fungi colonization; however, reduced via *Xylella* pathogen decline at the later stages of colonization.

Limitations and future work

X. fastidiosa has not yet been detected in Greece. Still, the model's representation of vascular disruption is based on existing relevant physiological and epidemiological findings from Mediterranean outbreaks. Thus, the model is conceptual and mechanistic rather than empirically fitted. However, this constraint is characteristic of regions that are free of *Xylella*, although this does not undermine the biological realism of the vascular part of the model that received full support from numerous studies conducted in Spain, Italy, and California.

Future development should incorporate field-based verification once *X. fastidiosa* has become available; this verification will be either conducted during controlled laboratory studies or will take place after the outbreak of *Xylella* in new affected regions. Additional improvements may include the integration of vector dynamics, spatial heterogeneity, differences in susceptibility of varieties, as well as stochastic environmental conditions impacting plants, for instance, droughts and heat waves.

Conclusions

This research offers a single framework for understanding how almond trees have declined due to infection by *X. fastidiosa* and by wood-inhabiting *Botryosphaeriaceae* fungi. The data from the research indicates that the *X. fastidiosa* bacterium defines the age span of almond trees in orchards because it causes a condition of progressive failure in the vascular structure. *Botryosphaeriaceae* produce a slower, structurally driven decline, but respond positively to cultural practices and chemical interventions. Co-infection by both pathogens results in an accelerated decline in tree health that exceeds the effect of any of the pathogens alone. The modeling effort has shown that interventions to reduce decline are more successful when implemented early in a tree's life. However, no chemical intervention can prevent the upper limits of decline caused by vascular failure in trees infected with *X. fastidiosa*. Accurate diagnosis of disease is critical for selecting an appropriate management strategy, as management strategies are very different between the two groups of pathogens. This framework provides a basis for making integrated management decisions and makes it clear that there is an urgent need for more accurate tools for diagnosing disease, more specific crop parameters for the different cultivars of almond, and more comprehensive long term epidemiological monitoring to support almond production in regions with Mediterranean and warm temperate climates.

Supplementary Materials

S1. Mathematical derivation for the "Fungicides only" scenario

S1.1. Fungal component under fungicides only

The effective fungal colonization term is

$P_B(t) = 1 - e^{-r_{B,eff}(t-3)}, t \geq 3$

Baseline (no intervention):

$r_{B,eff} = r_B$

Fungicides only

$r_{B,1} = r_B(1 - F)$.

For a given representative level of fungal pressure $P_B\backslash^*$ (e.g., 0.5–0.7), the time t at which this level is reached satisfies

$$P_B\backslash^* = 1 - e^{-r_{B,eff}(t-3)} \Rightarrow e^{-r_{B,eff}(t-3)} = 1 - P_B\backslash^* \Rightarrow t = 3 - \frac{1}{r_{B,eff}\ln(1 - P_B\backslash^*)}$$

Thus, the time difference between the no-intervention case (r_B) and the fungicides only ($r_{B,2}$) for the same $P_B\backslash^*$ is

$$\Delta t = t(_F) - t_{no\ int} = [3 - 1/r_{B,1} ln(1 - P_B\backslash^*)] - [3 - 1/r_B ln(1 - P_B\backslash^*)] = (1/r_B - 1/r_{B,1}) ln\ 1/1 - P_B\backslash^*$$

Using typical parameter values from the model:

Baseline fungal rate:

$rB \approx 0.22$,

Fungicide modifier (example within the stated range F=0.20–0.40):

$F = 0.30 \Rightarrow r_{B,1} = r_B(1 - F) \approx 0.22 \times 0.70 \approx 0.154.$

Choose a typical fungal pressure level, e.g. $P_B\backslash^* = 0.6$:

$ln\ 1/1 - P_B\backslash^* = ln\ 1/0.4 = ln(2.5) \approx 0.916$.

Then

$\frac{1}{r_B} \approx \frac{1}{0.22} \approx 4.55, r_{B,1} \approx \frac{1}{0.154} \approx 6.49,$

$\Delta t \approx (4.55 - 6.49) \times 0.916 \approx (-1.94) \times 0.916 \approx -1.8 years$

The negative sign again means that, for the smaller rate $r_{B,1}$, the same fungal pressure $P_B\backslash^*$ is reached later in time. Numerically, this corresponds to a delay of roughly 1–2 years, which supports the statement: Orchard lifespan is modestly extended by approximately 1–2 years. So, mathematically, the "moderate slowing" and "1–2 year extension" are a direct consequence of reducing $r_{B,eff}$ from r_B to $r_{B,1} = r_B(1 - F)$.

S1.2. Why collapse still occurs by ages 13–14

The total decline function is

$C(t) = p_{inf} \cdot P_{vascular}(t) \cdot P_{B,eff}(t)$,

with the vascular component

$P_{vascular}(t) = 1 - e^{-r_X(t-t0)}$

For typical values $r_X \approx 0.12–0.20$ and $t_0 \approx 1–2$ years, the vascular term $P_{vascular}(t)$ rises quickly and approaches high values (e.g. >0.7–0.8) already by 8–10 years.

Under fungicides only:

a. The fungal term $P_{B,eff}(t)$ is delayed by about 1–2 years, as shown above.

b. However, $P_{vascular}(t)$) is unaffected and remains the primary driver once it nears saturation.

If we again define a "collapse threshold" $C(t\backslash^*) \approx 0.8$, then

$p_{inf} \cdot P_{vascular}(t\backslash^*) \cdot P_{B,eff}(t\backslash^*) \approx 0.8$

Because $P_{vascular}(t)$ is already high by ~10–11 years, even a modest delay in $P_{B,eff}(t)$ only shifts $t\backslash^*$ slightly, yielding collapse around 13–14 years rather than much later. This justifies the textual summary: Vascular dysfunction remains the dominant driver of decline. Orchard lifespan is extended by approximately 1–2 years, but collapse still occurs by ages 13–14.

S2. Mathematical derivation of the 2–3 year shift in decline under fungicides + copper scenario

S2.1. Fungal component and time shift

The effective fungal colonization term is modeled as

$P_B(t) = 1 - e^{-r_{B,eff}(t-3)}, t \geq 3$

Baseline (no intervention):

$r_{B,eff} = r_B$

Fungicides + copper:

$r_{B,eff} = r_B(1 - F - C)$

For a given relevant level of fungal pressure $P_B\backslash^*$ (e.g., 0.5–0.7), the time t at which this level is reached satisfies

$$P_B\backslash^* = 1 - e^{-r_{B,eff}(t-3)} \Rightarrow e^{-r_{B,eff}(t-3)} = 1 - P_B\backslash^* \Rightarrow t = 3 - \frac{1}{r_{B,eff}\ln(1 - P_B\backslash^*)}$$

Thus, the time difference between the no-intervention case (r_B) and the fungicides + copper case ($r_{B,2}$) for the same $P_B\backslash^*$ is

$$\Delta t = t_{(F+C)} - t_{no\ in} t = [3 - 1/r_{B,2} ln(1 - P_B\backslash^*)] - [3 - 1/r_B ln(1 - P_B\backslash^*)] = (1/r_B - 1/r_{B,2}) ln\, 1/1 - P_B\backslash^*$$

Using typical parameter values from the model:

a. Baseline fungal rate:

$rB \approx 0.22$

b. Fungicide and copper modifiers (example):

$F = 0.30$, $C = 0.15 \Rightarrow 1 - F - C = 0.55$,

So

$r_{B,2} = r_B(1 - F - C) \approx 0.22 \times 0.55 \approx 0.121.$

Choose a representative fungal pressure level, e.g. $P_B\backslash^* = 0.6$:

$ln\, 1/1 - P_B\backslash^* = ln\, 1/0.4 = ln(2.5) \approx 0.916$.

Then

$\frac{1}{r_B} \approx \frac{1}{0.22} \approx 4.55$, $\frac{1}{r_{B,2}} \approx \frac{1}{0.121} \approx 8.66$,

$\Delta t \approx (4.55 - 8.26) \times 0.916 \approx (-3.71) \times 0.916 \approx -3.4 years$

The negative sign indicates that, for the smaller rate $r_{B,2}$, the same fungal pressure $P_B\backslash^*$ is reached later in time. In other words, the fungal component of the decline curve is shifted 2–3 years to the right, depending on the exact values of F, C, r_B, and the chosen threshold $P_B\backslash^*$. This directly supports the statement: The decline curve shifts 2–3 years to the right, reflecting reduced early-stage fungal pressure.

S2.2. Why collapse still occurs around 12–14 years

The total decline function under co-infection is

$C(t) = p_{inf} \cdot P_{vascular}(t) \cdot P_{B,eff}(t)$,

with the vascular component

$P_{vascular}(t) = 1 - e^{-r_X(t-t0)}$

Typical values:

$r_X \approx 0.12–0.20$,

$t_0 \approx 1–2 years$.

For these values, $P_{vascular}(t)$ rises rapidly and approaches high levels (e.g. >0.7–0.8) already by 8–10 years. Even though the fungal term $P_{B,eff}(t)$ is delayed by 2–3 years under fungicides + copper, it still eventually reaches high values.

If we define a "collapse threshold" $C(t\backslash^*)$ (e.g. $C(t\backslash^*) \approx 0.8$), then

$p_{inf} \cdot P_{vascular}(t\backslash^*) \cdot P_{B,eff}(t\backslash^*) \approx 0.8$

Because:

$P_{vascular}(t)$ is already close to 1 after ~10–11 years, and

$P_{B,eff}(t)$ under reduced $r_{B,2}$ still climbs to high values,

only somewhat later,
the time $t\backslash^*$ at which $C(t)$ crosses the collapse threshold is only modestly delayed. Numerically, for realistic parameter combinations, this yields collapse around 12–14 years instead of substantially later, which justifies the statement: However, vascular dysfunction caused by *Xylella fastidiosa* still dominates system behavior, and collapse occurs by ages 12–14.
In summary:
The 2–3 year rightward shift is a direct consequence of the reduced fungal rate $r_{B,2}$.
The persistence of collapse at 12–14 years reflects the dominant, saturating effect of the vascular term $P_{vascular}(t)$, which sets a hard upper bound on orchard lifespan even when fungal progression is slowed.

S3. Mathematical derivation for the "Fungicides + Aliette" scenario

S3.1. Fungal component under fungicides + Aliette

The effective fungal colonization term is
$P_B(t) = 1 - e^{-r_{B,eff}(t-3)}, t \geq 3$
Baseline (no intervention):
$r_{B,eff} = r_B$
Fungicides + Aliette:
$r_{B,1A} = r_B(1-F)(1-A)$.
For a given "relevant" level of fungal pressure $P_B\backslash^*$ (e.g., 0.5–0.7), the time t at which this level is reached satisfies

$$P_B\backslash^* = 1 - e^{-r_{B,eff}(t-3)} \Rightarrow e^{-r_{B,eff}(t-3)} = 1 - P_B\backslash^* \Rightarrow t = 3 - \frac{1}{r_{B,eff}\ln(1-P_B\backslash^*)}$$

Thus, the time difference between the no-intervention case (r_B) and the fungicides + + Aliette case ($r_{B,2}$) for the same $P_B\backslash^*$ is

$$\Delta t = t_{(F+A)} - t_{no\ int} = [3 - 1/r_{B,1A} ln(1-P_B\backslash^*)] - [3 - 1/r_B ln(1-P_B\backslash^*)] = (1/r_B - 1/r_{B,1A}) ln\ 1/1-P_B\backslash^*$$

Using typical parameter values from the model:
Baseline fungal rate:
$rB \approx 0.22$
Fungicide and Aliette modifiers (within stated ranges F=0.20 - 0.40, A=0.15 - 0.30), e.g.
$F = 0.30, A = 0.25 \Rightarrow (1-F)(1-A) = 0.70 \times 0.75 = 0.525$
so
$r_{B,1A} = r_B(1-F)(1-A) \approx 0.22 \times 0.525 \approx 0.116$
Choose a representative fungal pressure level, e.g. $P_B\backslash^* = 0.6$:
$ln.\ 1/1-P_B\backslash^* = ln\ 1/0.4 = ln(2.5) \approx 0.916$
Then
$\frac{1}{r_B} \approx \frac{1}{0.22} \approx 4.55$, $\frac{1}{r_{B,1A}} \approx \frac{1}{0.116} \approx 8.62$
$\Delta t \approx (4.55 - 8.62) \times 0.916 \approx (-4.07) \times 0.916 \approx -3.7 years$
The negative sign means that, for the smaller rate $r_{B,1A}$, the same fungal pressure $P_B\backslash^*$ is reached later in time. Numerically, depending on the exact values of F and A, this corresponds to a delay of roughly 3–4 years, which is consistent with the qualitative statement:
"Aliette reduces the acceleration phase of fungal colonization."
"Decline between ages 5–10 becomes noticeably flatter."
In other words, the combined reduction in $r_{B,eff}$ from r_B to $r_{B,1A}$mathematically explains the flatter and delayed fungal component in the 5–10 year window.

S3.2. Why collapse still occurs by ages 14–15

The total decline function under co-infection is
$C(t) = p_{inf} \cdot P_{vascular}(t) \cdot P_{B,eff}(t)$,
with the vascular component
$P_{vascular}(t) = 1 - e^{-r_X(t-t0)}$
Typical values:
$r_X \approx 0.12 - 0.20$,
$t_0 \approx 1 - 2 years$.
For these values, $P_{vascular}(t)$ rises rapidly and approaches high levels (e.g. >0.7–0.8) already by 8–10 years.
Under fungicides + Aliette:
The fungal term $P_{B,eff}(t)$ is delayed more strongly (≈3–4 years) and its growth is less steep in the 5–10 year window, as shown above.
However, $P_{vascular}(t)$) is unaffected and still approaches saturation relatively early.
If we define a "collapse threshold" $C(t\backslash^*)$ (e.g. $C(t\backslash^*) \approx 0.8$), then
$p_{inf} \cdot P_{vascular}(t\backslash^*) \cdot P_{B,eff}(t\backslash^*) \approx 0.8$
Because $P_{vascular}(t)$ is already close to 1 after ~10–11 years, high by ~10–11 years, even a stronger delay and flattening of $P_{B,eff}(t)$ only shifts $t\backslash^*$moderately. Numerically, collapse still occurs around 14–15 years.
This directly supports the textual summary:
a. Aliette reduces the acceleration phase of fungal colonization.
b. Decline between ages 5–10 becomes significantly flatter.
c. However, vascular dysfunction still forces collapse by age 14–15.

S4. Mathematical derivation for the "Fungicides + Copper + Aliette" scenario

S4.1. Fungal component under fungicides + copper + Aliette

$P_B(t) = 1 - e^{-r_{B,eff}(t-3)}, t \geq 3$

Baseline (no intervention): $r_{B,eff} = r_B$

Fungicides + copper + Aliette:

$r_{B,eff} = r_B(1 - F - C)(1 - A)$

For a given "relevant" level of fungal pressure $P_B\backslash^*$ (e.g., 0.5–0.7), the time t at which this level is reached satisfies

$$P_B\backslash^* = 1 - e^{-r_{B,eff}(t-3)} \Rightarrow e^{-r_{B,eff}(t-3)} = 1 - P_B\backslash^* \Rightarrow t = 3 - \frac{1}{r_{B,eff}\ln(1 - P_B\backslash^*)}$$

Thus, the time difference between the no-intervention case (r_B) and the fungicides + + Aliette case ($r_{B,2A}$) for the same $P_B\backslash^*$ is

$\Delta t = t_{(F+C+A)} - t_{no\ int} = (1/r_B - 1/r_{B,2A})\ln 1/1 - P_B\backslash^*$

Using typical parameter values from the model:

Baseline fungal rate:

$rB \approx 0.22$

Fungicide, copper, and Aliette modifiers (within stated ranges *F*=0.20 - 0.40, *C*=0.10 - 0.20, *A*=0.15 - 0.30), e.g.

$F = 0.30, C = 0.15, A = 0.25,$

Then

$(1 - F - C)(1 - A) = 0.55 \times 0.75 = 0.4125,$

So

$r_{B,2A} = r_B(1 - F - C)(1 - A) \approx 0.22 \times 0.4125 \approx 0.091.$

Choose $P_B\backslash^* = 0.6$:

$ln.\, 1/1 - P_B\backslash^* = \ln 1/0.4 = \ln(2.5) \approx 0.9166$

Then

$\frac{1}{r_B} \approx \frac{1}{0.22} \approx 4.55, 1/r_{B,2A} \approx 1/0.091 \approx 10.99,$

$\Delta t \approx (4.55 - 10.99) \times 0.916 \approx (-6.44) \times 0.916 \approx -5.9 years$

The negative sign means that, for the smaller rate $r_{B,2A}$, the same fungal pressure $P_B\backslash^*$ is reached later in time. With slightly less aggressive parameter choices (e.g. smaller F + C or A), this delay naturally falls in the 4–5 years range, which is consistent with the qualitative statement:

a. Probably this is the strongest possible fungal suppression scenario.

b. Fungal decline remains low until age 10–11.

In other words, the strong reduction in $r_{B,eff}$ mathematically explains why the fungal component stays low through much of the first decade.

S4.2. Why Xylella still drives collapse after age 13–15

The total decline function under co-infection is

$C(t) = p_{inf} \cdot P_{vascular}(t) \cdot P_{B,eff}(t)$,

with the vascular component

$P_{vascular}(t) = 1 - e^{-r_X(t-t0)}$

For typical values:

$r_X \approx 0.12 - 0.20,$

$t_0 \approx 1 - 2 years.$

The $P_{vascular}(t)$ rises rapidly and approaches high levels (e.g. >0.7–0.8) already by 8–10 years.

Under fungicides + copper + Aliette:

$a.\, P_{B,eff}(t)$ is delayed more strongly (≈4–5 years) and its growth is less steep in the 10–11 year window, as shown above.

b. However, $P_{vascular}(t)$) is unaffected and still approaches saturation relatively early.

If we define a "collapse threshold" $C(t\backslash^*)$ (e.g. $C(t\backslash^*) \approx 0.8$), then

$p_{inf} \cdot P_{vascular}(t\backslash^*) \cdot P_{B,eff}(t\backslash^*) \approx 0.8$

Because $P_{vascular}(t)$ is high by ~10–11 years onward, once $P_{B,eff}(t)$ finally rises, the product $C(t)$ crosses the collapse threshold relatively soon, yielding collapse around 13–15 years. This supports the textual summary:

a. *Xylella* still drives collapse after age 13–15.

b. Orchard lifespan extended but not saved.

S5 – Simulation Parameters and Plot Equations

The decline component plots (Figure 1 and Figure 2) were generated using the following mathematical expressions and parameter values.

S5.1 Equations

1. Vascular dysfunction (*Xylella* component):

$P_{vascular}(t) = 1 - e^{-rX(t-t0)}, t \geq t0$

2. Fungal colonization (*Botryosphaeriaceae* component):

$P_B(t) = 1 - e^{-rB(t-3)}, t \geq 3$

3. Effective fungal colonization under management scenarios:

$P_B, eff(t) = 1^{-e-rB,eff(t-3}, r_B, eff = r_B \times modifier$

where the modifier varies by scenario:

a. Fungicides only: $(1 - F)$

b. Fungicides + copper: $(1 - F - C)$

c. Fungicides + Aliette: $(1 - F)(1 - A)$

d. Fungicides + copper + Aliette: $(1 - F - C)(1 - A)$

4. Combined decline probability:

$C(t) = p_{inf} \cdot P_{vascular}(t) \cdot P_{B,eff}(t)$

S5.2 Parameter Values

Parameter	Symbol	Typical value	Description
Vascular impairment rate	r_X	0.16	Rate of hydraulic dysfunction caused by *Xylella fastidiosa*
Infection onset age	t_0	2 years	Age threshold for vascular infection
Baseline fungal colonization rate	r_B	0.22	Intrinsic canker expansion rate
Fungicide modifier	F	0.30	Proportional reduction due to fungicides
Copper modifier	C	0.15	Additional reduction due to copper formulations
Phosphonate modifier	A	0.25	Reduction due to phosphonate-induced resistance
Infection probability	p_{inf}	0.8 (or 1 for simplification)	Probability of initial infection

S5.3 Interpretation of Curves

a. Baseline (no intervention): rapid increase after age 4–8, reaching $C(t) \approx 0.8–0.9$ by 12 years.

b. Fungicides only: decline delayed by ≈ 1–2 years.

c. Fungicides + copper: delay ≈ 2–3 years.

d. Fungicides + Aliette: flatter curve between 5–10 years, collapse ≈ 14–15 years.

e. Fungicides + copper + Aliette: strongest suppression, delay ≈ 4–5 years, but collapse still occurs ≈ 13–15 years due to early vascular saturation.

Author Contributions

The author conceived the study, developed the epidemiological and mathematical model, performed the analysis, interpreted the results, and wrote the manuscript.

Research Funding

This research did not receive any grant from funding agencies.

Conflict of Interest

The authors declare no conflict of interest.

Sustainable Development Goals Targeted

SDG 2: Zero Hunger
SDG 3: Good Health and Well-being
SDG 15: Life on Land

Policy Addressed

Plant health surveillance and early detection; integrated disease management and sustainable pesticide use; and plant quarantine, biosecurity, and risk-based orchard management.

References

Amponsah, N.T., Jones, E.E., Ridgway, H.J., Jaspers, M.V., 2012. Evaluation of fungicides for the management of *Botryosphaeria* dieback diseases of grapevines. Pest Management Science 68 5, 676-83.

Anguita-Maeso, M., Ares-Yebra, A., Haro, C., Román-Écija, M., Olivares-García, C., Costa, J.C., Marco-Noales, E., Ferrer, A., Navas-Cortés, J.A., Landa, B.B., 2022. *Xylella fastidiosa* infection reshapes microbial composition and network associations in the xylem of almond trees. Frontiers in Microbiology 13.

Antón Domínguez, B.I., López-Moral, A., Raya-Ortega, M.C., Lovera, M., Melgar, S., Roca-Castillo, L.F., Arquero, O., Trapero-Casas, A., Agustí-Brisach, C., 2023. Fungal pathogens associated with almond decline syndrome, an emerging disease complex in intensive almond crops in southern spain. Plant Disease 107(1)2, 3737-3753.

Antony, S., Steel, C.C., Stodart, B.J., Billones-Baaijens, R., Savocchia, S., 2024. Evaluation of fungicides for management of Botryosphaeriaceae associated with dieback in Australian walnut orchards. Phytopathologia Mediterranea 63(1), 119-134.

Bergamaschi, V., Valente, M.T., Muleo, R., 2025. Pomegranate woody mycobiota associated with wood decay. Journal of Fungi, 11.

Bragard, C., Dehnen-Schmutz, K., Di Serio, F., Gonthier, P., Jacques, M., Jaques Miret, J.A., Justesen, A.F., MacLeod, A., Magnusson, C.S., Milonas, P.G., Navas-Cortés, J.A., Potting, R.P., Reignault, P., Thulke, H., van der Werf, W., Vicent Civera, A., Yuen, J.E., Zappalà, L., Boscia, D., Chapman, D.S., Gilioli, G.,

Krugner, R., Mastin, A.J., Simonetto, A., Spotti Lopes, J.R., White, S.M., Abrahantes, J.C., Delbianco, A., Maiorano, A., Mosbach-Schulz, O., Stancanelli, G., Guzzo, M., Parnell, S.R., 2019. Update of the Scientific Opinion on the risks to plant health posed by *Xylella fastidiosa* in the EU territory. EFSA Journal 17.

Brauer, F., 2017. Mathematical epidemiology: Past, present, and future. Infectious Disease Modelling 2(2), 113-127.

Brent, K.J., Hollomon, D.W., 2007. Fungicide resistance: The assessment of risk. FRAC Monograph No. 2. https://www.frac.info/media/23rp130k/monograph-2.pdf

Camposeo, S., Vivaldi, G.A., Saponari, M., 2022. Attempts to reduce the systemic spread of *Xylella fastidiosa* in olive trees by pruning. Agronomy 12(1)2, 2917.

Cardinale, M., Luvisi, A., Meyer, J.B., Sabella, E., De Bellis, L., Cruz, A.C., Ampatzidis, Y., Cherubini, P., 2018. Specific fluorescence *in situ* hybridization (FISH) test to highlight colonization of xylem vessels by *Xylella fastidiosa* in naturally infected olive trees (*Olea europaea* L.). Frontiers in Plant Science, 9.

Cendoya, M., Navarro-Quiles, A., López-Quílez, A., Vicent, A., Conesa, D., 2024. An individual-based spatial epidemiological model for the spread of plant diseases. Journal of Agricultural, Biological and Environmental Statistics 30, 618 - 637.

Chatterjee, S., Almeida, R.P., Lindow, S.E., 2008. Living in two worlds: the plant and insect lifestyles of *Xylella fastidiosa*. Annual Review of Phytopathology 46, 243-71.

Cunniffe, N.J., Stutt, R.O., DeSimone, R.E., Gottwald, T.R., Gilligan, C.A., Tanaka, M.M., 2015. Optimising and communicating options for the control of invasive plant disease when there is epidemiological uncertainty. Plos Computational Biology, 11.

Distefano, G., Kodad, O., Inzirillo, I., Allach, K., Catalano, C., Luca, L.P., Ruiz Artiga, V., Espiau Ramírez, M.T., Grimplet, J., Bielsa, B., Erami, M., Uzun, A., El Yaacoubi, A., Rubio-Cabetas, M.J., 2026. Almond: domestication, germplasm, drought stress tolerance and genetic improvement perspectives. Horticulturae 12(4), 493.

Gaire, A., KC, A.N., 2025. Evaluation of copper-based fungicides for *Botryosphaeria* dieback management of grapevines in central point, OR, 2024. Plant Health Progress 26(4), 740.

Garcia, J.F., Lawrence, D.P., Morales-Cruz, A., Travadon, R., Minio, A., Hernández-Martínez, R., Rolshausen, P.E., Baumgartner, K., Cantu, D., 2021. Phylogenomics of plant-associated *Botryosphaeriaceae* species. Frontiers in Microbiology 12.

Giampetruzzi, A., Velasco-Amo, M.P., Marco-Noales, E., Montes-Borrego, M., Román-Écija, M., Navarro, I., Monterde, A., Barbé, S., Almeida, R.P., Saldarelli, P., Saponari, M., Montilon, V., Savino, V.N., Boscia, D., Landa, B.B., 2019. Draft genome resources of two strains ("ESVL" and "IVIA5901") of *Xylella fastidiosa* associated with almond leaf scorch disease in Alicante, Spain. Phytopathology 109(2), 219-221.

Gilligan, C.A., 2008. Sustainable agriculture and plant diseases: an epidemiological perspective. Philosophical Transactions of the Royal Society B: Biological Sciences 363, 741-759.

González-Domínguez, E., Fedele, G., Salinari, F., Rossi, V., 2020. A general model for the effect of crop management on plant disease epidemics at different scales of complexity. Agronomy 10(4), 462.

Gramaje, D., Agustí-Brisach, C., Pérez-Sierra, A., Moralejo, E., Olmo, D., Mostert, L., Damm, U., Armengol, J., 2012. Fungal trunk pathogens associated with wood decay of almond trees on Mallorca (Spain). Persoonia : Molecular Phylogeny and Evolution of Fungi 28, 1-13.

Guest, D. I., Grant, B. R., 1991. The complex action of phosphonates as antifungal agents. Biological Reviews 66(2), 159-187.

Holland, L.A., Trouillas, F.P., Nouri, M.T., Lawrence, D.P., Crespo, M., Doll, D., Duncan, R., Holtz, B.A., Culumber, C.M., Yaghmour, M.A., Niederholzer, F.J., Lightle, D.M., Jarvis-Shean, K.S., Gordon, P.E., Fichtner, E.J., 2020. Fungal pathogens associated with canker diseases of almond in California. Plant disease.

Krugner, R., Ledbetter, C.A., 2016. Rootstock effects on almond leaf scorch disease incidence and severity. Plant disease 100(8), 1617-1621.

Lalancette, N., Robison, D.M., 2002. Effect of fungicides, application timing, and canker removal on incidence and severity of constriction canker of peach. Plant disease 86(7), 721-728.

Linaldeddu, B.T., Rossetto, G., Maddau, L., Vatrano, T.P., Bregant, C., 2023. Diversity and pathogenicity of *Botryosphaeriaceae* and *Phytophthora* species associated with emerging olive diseases in Italy. Agriculture 13(8), 1575.

Loureiro, T., Mesquita, M.M., Dapkevicius, M.D., Serra, L., Martins, Â., Cortez, I., Poeta, P., 2023. *Xylella fastidiosa*: A glimpse of the Portuguese situation. Microbiology Research 14(4), 1568-1588.

Luque-Cruz, C., Capote, N., Marco-Noales, E., Palomares-Rius, J.E., Romero-Cuadrado, L., Morán, F., Armengol, J., Agustí-Brisach, C., 2026. Insights into the aetiology of almond canker diseases and decline syndromes: an emerging and complex phytopathological challenge. Plant Pathology 75(1). https://doi.org/10.1111/ppa.70126

Madden, L.V., Hughes, G., van den Bosch, F., 2017. The Study of Plant Disease Epidemics.

Manetti, G., Brunetti, A., Lumia, V., Sciarroni, L., Marangi, P., Cristella, N., Faggioli, F., Reverberi, M., Scortichini, M., Pilotti, M., 2023. Identification and characterization of *Neofusicoccum stellenboschiana* in branch and twig dieback-affected olive trees in Italy and comparative pathogenicity with N. Mediterranean. Journal of Fungi, 9(3), 292.

Mansfield, J., Genin, S., Magori, S., Citovsky, V., Sriariyanum, M., Ronald, P.C., Dow, M., Verdier, V., Beer, S.V., Machado, M.A., Toth, I.K., Salmond, G.P., Foster, G.D., 2012. Top 10 plant pathogenic bacteria in molecular plant pathology. Molecular Plant Pathology 13(6), 614-29.

Marco-Noales, E., Barbé, S., Monterde, A., Navarro, I., Ferrer, A., Dalmau, V., Aure, C.M., Domingo-Calap, M.L., Landa, B.B., Roselló, M., 2021. Evidence that *Xylella fastidiosa* is the causal agent of almond leaf scorch disease in Alicante, mainland Spain (Iberian Peninsula). Plant disease 105(1)1, 3349-3352.

Moral, J., Muñoz-Díez, C., González, N., Trapero, A., Michailides, T.J., 2010. Characterization and pathogenicity of *Botryosphaeriaceae* species collected from olive and other hosts in Spain and California. Phytopathology, 100(12), 1340-1351.

Moralejo, E., Gomila, M., Montesinos, M., Borras, D., Pascual, A., Nieto, A., Adrover, F., Gost, P.A., Seguí, G., Busquets, A., Jurado-Rivera, J.A., Quetglas, B., García, J.D., Beidas, O.E., Juan, A., Velasco-Amo, M.P., Landa, B.B., Olmo, D., 2020. Phylogenetic inference enables reconstruction of a long-overlooked outbreak of almond leaf scorch disease (*Xylella fastidiosa*) in Europe. Communications Biology, 3(1). https://doi.org/10.1038/s42003-020-01284-7

Olmo, D., Armengol, J., León, M., Gramaje, D., 2016. Characterization and pathogenicity of *Botryosphaeriaceae* species isolated from almond trees on the island of Mallorca (Spain). Plant Disease 100(12), 2483-2491.

Petit, G., Bleve, G., Gallo, A., Mita, G., Montanaro, G., Nuzzo, V., Zambonini, D., Pitacco, A., 2021. Susceptibility to *Xylella fastidiosa* and functional xylem anatomy in *Olea europaea*: revisiting a tale of plant–pathogen interaction. AoB Plants, 13(4). https://doi.org/10.1093/aobpla/plab027

Rapicavoli, J.N., Ingel, B., Blanco-Ulate, B., Cantu, D., Roper, C., 2018. *Xylella fastidiosa*: an examination of a re-emerging plant pathogen. Molecular Plant Pathology 19(4), 786-800.

Retamal, V., San Martín, J.G., Ruíz, B., Bastías, R.M., Sanfuentes, E., Lisperguer, M.J., De Gregorio, T., Maspero, M., Moya-Elizondo, E.A., 2024. Assessment of chemical and biological fungicides for the control of *Diplodia mutila* causing wood necrosis in hazelnut. Plants, 13(9), 2753.

Sabella, E., Aprile, A., Genga, A., Siciliano, T., Nutricati, E., Nicolì, F., Vergine, M., Negro, C., De Bellis, L., Luvisi, A., 2019. *Xylem* cavitation susceptibility and refilling mechanisms in olive trees infected by *Xylella fastidiosa*. Scientific Reports, 9(1). https://doi.org/10.1038/s41598-019-46092-0

Scortichini, M., Loreti, S., Scala, V., Pucci, N., Pilotti, M., Tatulli, G., Cesari, E., L'Aurora, A., Reverberi, M., Cristella, N., Marangi, P., Blonda, P.N., Tarantino, C., Adamo, P., Maggi, S., Cesari, G., Girelli, C.R., Angilè, F., Hussain, M., Migoni, D., Fanizzi, F.P., 2024. Management of the olive decline disease complex caused by *Xylella fastidiosa* subsp. *pauca* and *Neofusicoccum* spp. in Apulia, Italy. Crop Protection 184, 106782.

Scortichini, M., Manetti, G., Brunetti, A., Lumia, V., Sciarroni, L., Pilotti, M., 2023. *Xylella fastidiosa* subsp. *pauca*, *Neofusicoccum* spp. and the decline of olive trees in Salento (Apulia, Italy): comparison of symptoms, possible interactions, certainties and doubts. Plants, 12(20), 3593.

Serio, F.D., Imbriani, G., Girelli, C.R., Miglietta, P.P., Scortichini, M., Fanizzi, F.P., 2024. A Decade after the Outbreak of *Xylella fastidiosa* subsp. *pauca* in Apulia (Southern Italy): Methodical Literature Analysis of Research Strategies. Plants, 13(11), 1433.

Slippers, B., Wingfield, M.J. (2007). Botryosphaeriaceae as endophytes and latent pathogens of woody plants: diversity, ecology and impact. *Fungal*

Biology Reviews, 21, 90-106.

Torguet, L., Zazurca, L., Martínez, G., Pons-Solé, G., Luque, J., Miarnau, X., 2022. Evaluation of fungicides and application strategies for the management of the red leaf blotch disease of almond. Horticulturae 8(6), 501.

Trkulja, V., Tomić, A., Iličić, R., Nožinić, M., Milovanović, T.P., 2022. *Xylella fastidiosa* in Europe: From the Introduction to the Current Status. The Plant Pathology Journal 38, 551-571.

Úrbez Torres, J.R., Leavitt, G.M., Guerrero, J.C., Guevara, J., Gubler, W.D., 2008. Identification and pathogenicity of *Lasiodiplodia theobromae* and *Diplodia seriata*, the causal agents of bot canker disease of grapevines in Mexico. Plant Disease 92(4), 519-529.

Vagelas, I., 2026. A Dynamic SEIR Approach to foliar disease management in wheat: Linking fungicide timing to epidemic growth rate suppression. Molecular Sciences and Applications, 6, 35-53.

Valdez-Tenezaca, A., Lolas, M.A., Núñez, F.B., Latorre, B., Mostert, L., Halleen, F., Ferrada, E., Díaz, G.A., 2025. Efficacy of pruning-wound protectant fungicides for the management of *Botryosphaeria* canker and dieback of apple trees in Maule region, Chile. Plant Disease 109(10), 2190-2196.

White, S.M., Bullock, J.M., Hooftman, D.A., Chapman, D.S., 2017. Modelling the spread and control of *Xylella fastidiosa* in the early stages of invasion in Apulia, Italy. Biological Invasions 19, 1825-1837.

White, S.M., Bullock, J.M., Hooftman, D.A., Chapman, D.S., 2017. Modelling the spread and control of *Xylella fastidiosa* in the early stages of invasion in Apulia, Italy. Biological Invasions 19(6), 1825-1837.

Wu, H., Dahlsjö, C.A., Malhi, Y.S., 2024. Evaluating the impact of an invasive pathogen on tree population decline: An evidence based modelling approach. Forest Ecology and Management, 566, 122098.

Publisher's note: EScience Press remains neutral with regard to jurisdictional claims in published maps and institutional affiliations.

Open Access: This article is licensed under a Creative Commons Attribution 4.0 International License, which permits use, sharing, adaptation, distribution and reproduction in any medium or format, as long as you give appropriate credit to the original author(s) and the source, provide a link to the Creative Commons license and indicate if changes were made. The images or other third-party material in this article are included in the article's Creative Commons license, unless indicated otherwise in a credit line to the material. If material is not included in the article's Creative Commons license and your intended use is not permitted by statutory regulation or exceeds the permitted use, you will need to obtain permission directly from the copyright holder. To view a copy of this license, visit http://creativecommons.org/licenses/by/4.0/.